E-proceedings of the 38th IAHR World Congress
September 1-6, 2019, Panama City, Panama
doi:10.3850/38WC092019-0909

A STOCHASTIC BUBBLE GENERATOR FOR AIR-WATER FLOW RESEARCH

DANIEL VALERO[(1)], MATTHIAS KRAMER[(2)], DANIEL B. BUNG[(3)] & HUBERT CHANSON[(4)]

[(1)] IHE Delft Institute for Water Education, Water Science and Engineering, Delft, the Netherlands
d.valero@un-ihe.org

[(2)] University of New South Wales, School of Engineering and Information Technology, Canberra, Australia
m.kramer@adfa.edu.au

[(3)] Aachen University of Applied Sciences, Hydraulic Engineering Section, Aachen, Germany
bung@fh-aachen.de

[(4)] The University of Queensland, School of Civil Engineering, Brisbane, Australia
h.chanson@uq.edu.au

ABSTRACT

Highly turbulent free-surface flows are often characterized by air entrainment, resulting in considerable flow bulking and a modulation of energy dissipation. An understanding of air-water flows remains constrained by instrumentation limitations, scale effects and few analytical developments. Whereas past attempts have addressed air-water flow research from a deterministic point of view, this work expands recent studies by developing a three-dimensional stochastic model for the simulation of bubble kinematics. The model is based on mean and turbulent velocity properties of turbulent boundary layers, being of interest for the study of aerated free-surface flows and the validation of measurement instrumentation. A verification of the code is presented, accompanied by a discussion of limitations and future research opportunities.

Keywords: Multiphase turbulence, turbulence estimations, shear flow, spillway, boundary layer, bubble kinematics

1 INTRODUCTION

Air bubble entrainment oftentimes occurs in highly turbulent free-surface flows, as those in hydraulic structures and environmental flows. Well-known examples are spillways (Wood 1984, Chanson 1994, Boes and Hager 2003, Bung 2011), hydraulic jumps (Chanson and Brattberg 2000, Murzyn et al. 2005, Wang et al. 2015) and coastal waves (Deane and Stokes 2002). Since the early work of Straub and Anderson (1958), the majority of air-water flow research has been conducted using physical models, involving deterministic approaches and experimental data (Chanson 1996, Wei et al. 2016, Valero and Bung 2016, Kramer et al. 2018, Valero and Bung 2018).

Figure 1. Air-water flows in human-made and natural environments. Left: steady jump in Eisbach, Munich, Germany (October 2018); right: waterfall in Cañete, Spain (March 2018).

Several seminal questions are yet to be addressed, e.g.: how accurate are experimental techniques in detecting interfacial velocities? In contrast to single-phase flows, analytical derivations are scarce and there is limited data for comparison across experimental techniques. Recently, Bung and Valero (2017) and Kramer et al. (2019b) used stochastic signals to explore limitations of experimental techniques in aerated flows. The basic idea involves the simulation of the motion of particles (droplets or bubbles) with realistic velocity fields. The position of these particles is updated every time step, allowing to evaluate the response of flow measurement instrumentation. Bung and Valero (2017) generated moving particles of different sizes over a black background, aiming to simulate high-speed camera images. The synthetic images also included light effects and were used to assess the performance of image-based velocimetry methods such as Optical Flow. A direct quantification of the measurement error was possible as the "true" velocities of the particles were known. Similarly, Kramer et al. (2019b) generated velocity signals in one dimension, which were applied to synthetic particles following a certain size distribution. The response of a dual-tip phase-detection probe was simulated by generating "virtual" time series for each tip, and the measurement uncertainty of a novel signal processing technique (adaptive window cross-correlation, AWCC) was evaluated. The AWCC technique allows the estimation of pseudo-instantaneous velocities and the comparison of measured velocities with "true" velocities confirmed capabilities to estimate direct turbulent quantities in highly aerated flows.

In addition to instrumentation limitations, air-water flows may be subjected to scale effects (Chanson 2009, Felder and Chanson 2017) and a vacuum of large-scale measurements has resulted in a lack of fundamental understanding. Large uncertainties are also associated to numerical methods in the field of aerated flows (Bombardelli 2012, Valero and Bung 2015, Valero and García-Bartual 2016, Castro et al. 2016). Overall, the understanding of air-water flows lags behind that of single-phase flows (Chanson 2013). The development of stochastic tools for the study of bubble kinematics aims to advance the current knowledge and provides a basis for more complex physics modelling. It further allows the testing of theories and simulation results can be compared to experimental data, shedding possibly some light on the turbulent flow structure and phenomena such as turbulence modulation.

In this study, the stochastic model developed by Bung and Valero (2017) and Kramer et al. (2019b) is expanded to three-dimensions. Given the lack of knowledge on turbulence properties in highly aerated flows, turbulence statistics are modelled based upon semi-analytical solutions for the single-phase turbulent boundary layer flow on a spillway. The equations of the stochastic bubble generator including boundary layer equations are detailed in Sections 2 and 3. Section 4 presents the verification of the implementation in bubbly flows and the limitations of the approach are discussed in Section 5.

2 STOCHASTIC BUBBLE GENERATOR (SBG)

Let x_i be the space coordinate (with $i = x, y, z$) and t the time coordinate. The displacement of a bubble will be given by:

$$\frac{\mathrm{d}x_i}{\mathrm{d}t} \equiv U_i(t, x_i) \qquad [1]$$

being U_i the instantaneous velocity, that can be decomposed into its mean $\mathcal{U}_i$ and fluctuating u_i components as:

$$U_i(t, x_i) = \mathcal{U}_i\,(x_i) + u_i(t, x_i) \qquad [2]$$

In the following, the dependence on the space coordinate x_i is dropped for the sake of simplicity. The mean component has been widely reported in literature for different types of flows. Oftentimes, analytical solutions for basic shear flows are available. However, the analysis of fluctuating components is more complicated and their description is mainly derived from physical modelling. Following Eq. [2], the mean value of u is null by definition and it is common to find relationships based on its mean squared value.

For the sake of simulating the kinematics of bubbles subject to a turbulent velocity field, the velocity fluctuation will be modelled as a Brownian motion following the Langevin equation (Langevin 1908, Pope 2000):

$$\mathrm{d}u_i(t) = -u_i(t)\frac{\mathrm{d}t}{T_i} + \left(\frac{2{\sigma_i}^2}{T_i}\right)^{\frac{1}{2}}\mathrm{d}W(t) \qquad [3]$$

where σ_i is the scale of the velocity fluctuation and T_i is the characteristic time scale of the stochastic process, defined by the velocity autocorrelation function $\rho_i(s) = \exp(-s/T_i)$:

$$T_i = \int_0^{\infty} \rho_i(s)\, \mathrm{d}s \qquad [4]$$

and W represents a Wiener process. Eq. [3] is a stochastic differential equation, which can be approximated through finite differences as (Pope 2000):

$$u_i(t + \Delta t) = u_i(t) - u_i(t)\frac{\Delta t}{T_i} + \left(\frac{2{\sigma_i}^2 \Delta t}{T_i}\right)^{\frac{1}{2}} \xi(t) \qquad [5]$$

with $\xi(t)$ being a standardized Gaussian random variable. Eq. [3] (and [5]) is a diffusion equation, consistent with Kolmogorov (1941) for the inertial subrange. It is noteworthy that the first component on the RHS of Eq. [3] is an inertial term which tends to null the velocity fluctuation, proportionally to its magnitude value, whereas the second term corresponds to a random component.

3 BOUNDARY LAYER FLOW

Air-water mixtures can be found in different types of shear flows, including spillway flows, plunging jets and hydraulic jumps. Such types of flows are similar to the following single-phase flow cases: isotropic turbulence, boundary layer or free shear flows. Boundary layers occur in spillway flows. Downstream of the inception point, large quantities of air are entrained, and it can be expected to observe changes in turbulence quantities (Wood 1984, Chanson 1996). Despite the change of flow properties due to bubbles, i.e. turbulence modulation (Balachandar and Eaton 2010), it might be reasonable to use a single-phase flow description as a case study. In order to use SBG to reproduce the bubbles dynamics, some estimate of $\mathcal{U}_i$, σ_i and T_i must be developed, based upon boundary layer flows herein.

When a viscous fluid meets a solid surface, the no-slip condition leads to a velocity gradient, resulting on a boundary layer flow. It has been well-established that velocity profiles in spillway flows can be reproduced by the equation (Castro-Orgaz 2010):

$$\frac{\mathcal{U}_x}{u_*} = \frac{1}{\kappa}\ln\left(\frac{y}{k_s}\right) + B + \frac{1}{\kappa}(1 + 6\Pi)\left(\frac{y}{\delta}\right)^2 - \frac{1}{\kappa}(1 + 4\Pi)\left(\frac{y}{\delta}\right)^3 \qquad [6]$$

with $u_* = (\tau_0/\rho)^{1/2}$ the shear velocity, τ_0 the wall shear, ρ the fluid density, $\kappa = 0.41$ the von Kármán constant, $B = 8.5$ for turbulent rough channel flow, $\Pi = 0.2$ the wake parameter for spillway flows (following Castro-Orgaz 2010), k_s the sand roughness coefficient and δ the boundary layer thickness. The wall shear can be related to the free stream velocity (u_{fs}) and the skin friction coefficient (C_f) as:

$$\tau_0 = \frac{1}{2}\rho C_f {u_{fs}}^2 \qquad [7]$$

Castro-Orgaz (2010) provided an expression for the skin friction coefficient in spillway flows:

$${C_f}^{-1/2} = 3.967 \log\left(\frac{\delta}{k_s}\right) + 6.7 \qquad [8]$$

with common k_s values in the order of 1 to 1.5 mm for smooth concrete spillways. The shear velocity is related to the skin friction coefficient as follows:

$$u_* = u_{fs}\sqrt{\frac{C_f}{2}} \qquad [9]$$

Velocity fluctuations are generated due to the shearing at the wall surface and are expected to scale with u_*. The semi-empirical expression proposed by Nezu (1977) can be used to estimate the scale of the streamwise, vertical and spanwise velocity fluctuations σ_x, σ_y, and σ_z, respectively, in the range $0.10 < y/\delta < 1$:

$$\frac{\sigma_i}{u_*} = D_i \exp\left(-K_i \frac{y}{\delta}\right) \qquad [10]$$

being D_i and K_i model coefficients. Valero (2018) conducted a literature review, proposing coefficients D_i and K_i based on the experimental data of Cameron et al. (2017) [Table 1 and Fig. 2].

Table 1. Model coefficients for equation [10] based on the experimental data of Cameron et al. (2017), following a fit of Valero (2018). R^2 is the coefficient of determination

	STREAMWISE		NORMALWISE		SPANWISE	
	D_x	K_x	D_y	K_y	D_z	K_z
BEST FIT	2.22	0.84	1.11	0.66	1.35	0.69
MINIMUM	2.18	0.80	1.06	0.58	1.33	0.65
MAXIMUM	2.26	0.88	1.15	0.75	1.38	0.73
R^2	0.983		0.978		0.898	

The computation of velocity time series with Langevin equation (Eq. [5]) is based on integral time scales of the flow, which were estimated as $T_i \approx L_i/\mathcal{U}_i$. It is proposed that the length scale for the streamwise direction L_x is proportional to the free path to the wall:

$$L_x = K_L\, y \qquad [11]$$

According to Pope (2000) and Tennekes and Lumley (1972), the transverse length scales $L_y = L_z = 0.5\, L_x$. In order to satisfy the experimental observations of Johnson and Cowen (2016) at the free surface level, $K_L \approx 1$. These integral length scales may be understood as a measure of the average eddy size, although a wide range of eddies are present in the flow.

4 VERIFICATION

The Stochastic Bubble Generator (SBG) equations were implemented in MATLAB. To verify the implementation of the basic equations, a given number of particles were randomly generated inside a control volume of extension δ^3 and equal sides. The lower 10 percent of the boundary layer thickness was initially empty, as Eq. [10] is not valid in the region next to the wall (see Figure 2). Nonetheless, some particles may enter that region due to unrestricted turbulent fluctuations. The boundaries of the control volume were implemented as a continuative condition, where bubbles passing the positive (negative) limit were automatically spawned at the opposed negative (positive) limit. Initially, the velocity of the particles followed the mean velocity (Eq. [6]). The particle sizes and distribution represented monodisperse bubbles with uniform air concentration, used to test the implementation of the SBG equations and to verify the bubble kinematics.

Several combinations of u_{fs}, δ, and k_s were tested as part of the verification. An example of generated bubbles and the control volume is presented in Figure 3. Turbulence statistics of the stochastic particles are presented in Figure 4 for one of the test cases. It must be noted that some diffusion is present in Figure 4 as the turbulence statistics are computed for the final position of the particles. However, the particles were travelling across the vertical direction, being affected by turbulence levels at other layers of the flow. Mean velocity profiles were also satisfactorily reproduced.

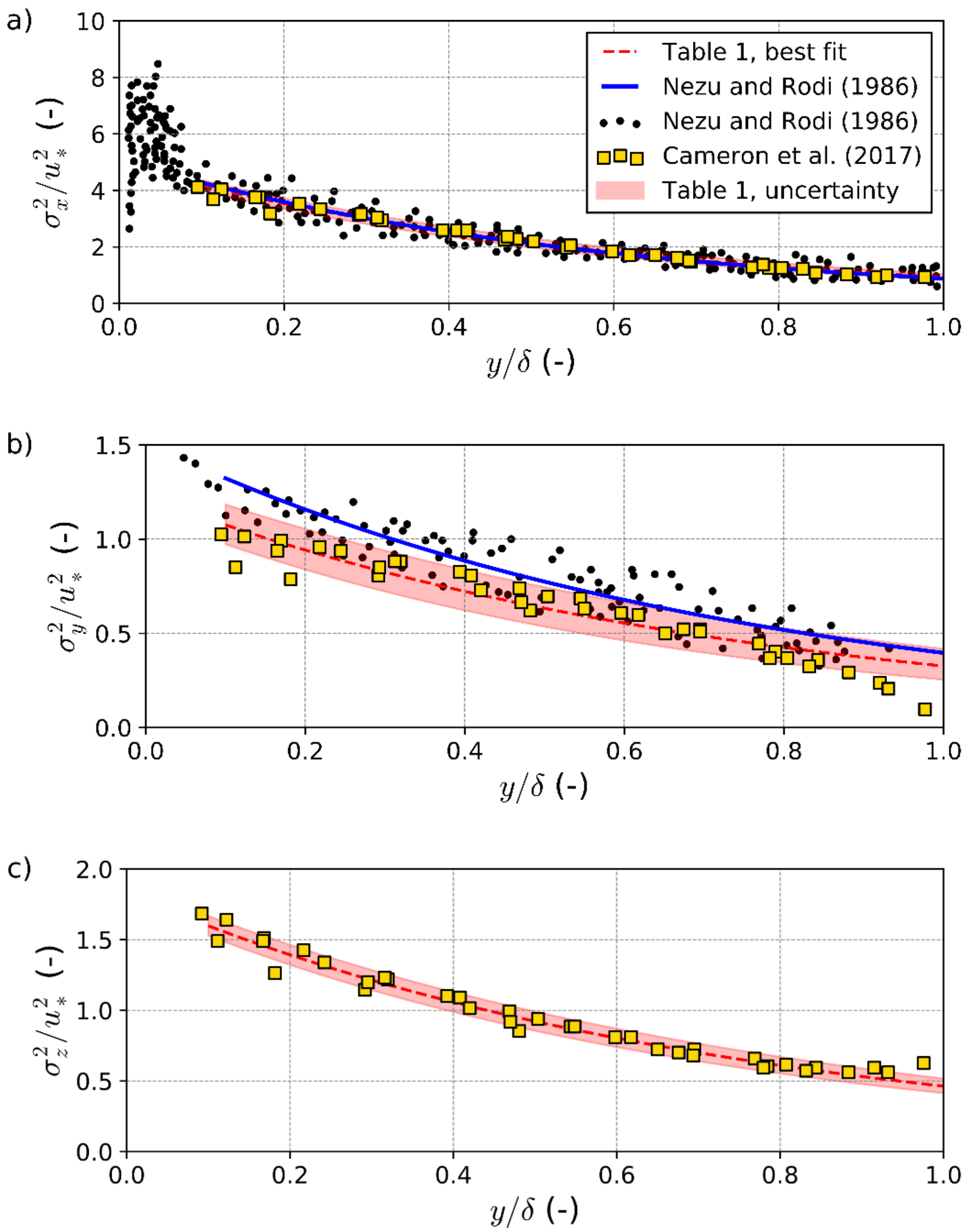

Figure 2. Scale of the velocity fluctuations from experimental data and Eq. [10] (Nezu 1977), together with coefficients of Table 1 for: a) streamwise, b) normalwise and c) spanwise velocity fluctuations. Data of Nezu and Rodi (1986) included for comparison. Figure adapted from Valero (2018).

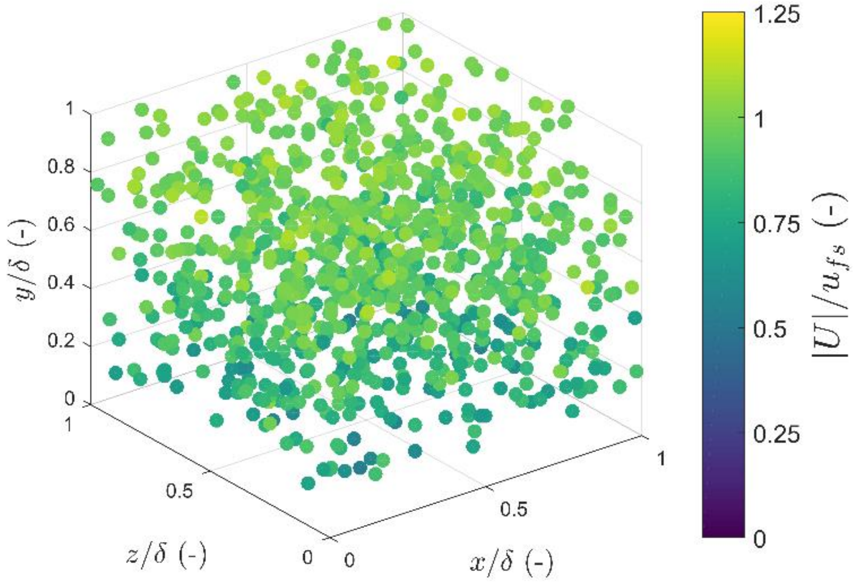

Figure 3. A thousand bubbles of 5 mm diameter generated inside the boundary layer flow (δ = 0.15 m). Color scale for the velocity magnitude $|U| = \sqrt{U_x{}^2 + U_y{}^2 + U_z{}^2}$. Mean air concentration of roughly 2 %.

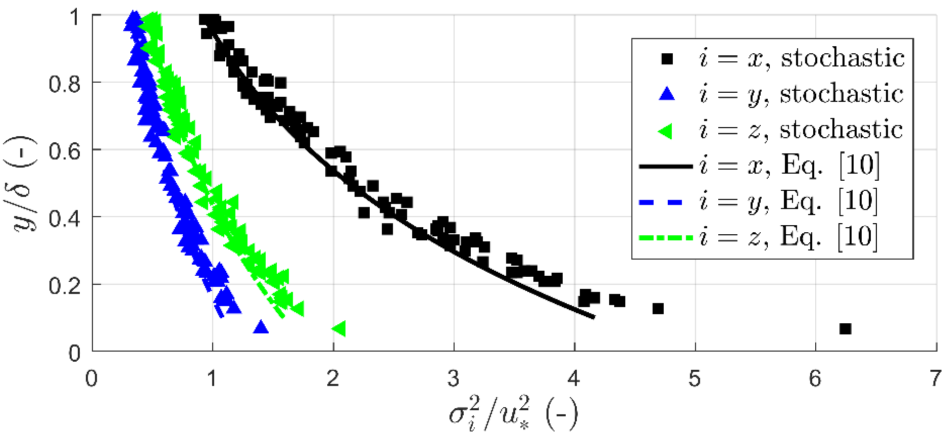

Figure 4. Turbulence quantities of the stochastic bubbles after 10 s of simulation for 100 bubbles of diameter 5 mm, integration with time step 1 ms. Free stream velocity u_{fs} = 3.3 m/s, boundary layer thickness δ = 0.15 m, and sand roughness coefficient k_s = 1.5 mm.

5 LIMITATIONS

The implemented stochastic bubble generator (SBG) adds new functionalities, when compared to the original works of Bung and Valero (2017) and Kramer et al. (2019b). Yet the SBG contains a number of limitations, including:

1. Homogeneous air concentration. Semi-theoretical air concentration profiles such as those of Wood (1984), Chanson (1996) or Chanson and Toombes (2002) could yield improved stochastic modelling. This would require a more sophisticated positioning of the bubbles, and incorporation of buoyancy to keep the profile steady.
2. Every bubble moves independently of the others, i.e. not inside the same coherent structure but as independent eddies of the size of the bubble.
3. The air-water flow structure consists of a dispersed phase, no mixture of bubbles and droplets nor other complex air-water structures (e.g. Felder and Chanson, 2016). Inclusion of an entrapped air concentration profile, such as observed in Valero and Bung (2016), and three-dimensional observations of the upper layer of the flow (Kramer et al. 2019a) may help distinguishing the zone where either

bubbles or droplets should be generated. Apart from that, more knowledge from experimental works is necessary to solve this issue.

4. A constant bubble size is assumed. The assumption is untrue as shown by the available literature (Chanson and Toombes 2002, Kramer et al. 2019b).
5. Velocity fluctuations are uncorrelated, which means that no turbulent shear stresses are included. This issue can be addressed by linking part of the bubble velocity variability in y to the variability of x, thus having a non-zero correlation.
6. No wall nor free surface effects are incorporated in this model. Bubbles can trespass the free surface or the wall, being simply placed in the opposed contour. No blockage effect, no-slip condition or entrainment/detrainment of bubbles is considered.
7. No bubble-bubble interaction. Bubbles approach other bubbles without modifying their trajectories (clustering) nor producing coalescence.

6 CONCLUSION AND FUTURE RESEARCH

In this study, a stochastic bubble generator (SBG) has been expanded to three-dimensional turbulent boundary layer flows. The well-accepted formulation for the non-aerated region (Castro-Orgaz 2010) has been applied to the aerated region. Since relatively little is known about direct estimations of turbulence quantities in air-water flows, the data of Cameron et al. (2017) on turbulent boundary layers were used. The SBG code was verified in Section 4, and limitations were discussed in Section 5.

Stochastic tools have been used in underground transport modelling, contaminant transport and general hydraulics. Up to now, little efforts have been made to explore its capabilities for air-water flow research. The use of moving bubbles with perfectly known positions and velocities may allow to approach relevant open research questions, for example:

1. Measurement accuracy of phase-detection probes (Kramer et al. 2019b) and other experimental methodologies (Bung and Valero 2017)
   a. Phase-detection probes: to determine the measurement accuracy, a virtual probe is placed inside the control volume and the interaction of the probe-tips with bubbles is simulated. This may allow studying the uncertainty of experimental data for different flow conditions and will help to optimize the design of phase-detection probes.
   b. Optical methods: image-based velocimetry can be tested but imaging effects (such as shadows, lights and erroneous pixels) must be incorporated (Bung and Valero 2017). This is challenging as light reflection and refraction at the air-water interphase behave non-linearly.
2. Fundamental insights. Since experimental datasets on bubble chords, clustering and interparticle arrival times are available (Chanson 2013), similar data can be extracted from the stochastic bubbles and fundamental physics can be added to reproduce the empirical data. This may allow testing different hypotheses on the air-water flow fluid mechanics.

REFERENCES

Balachandar, S. and Eaton, J.K. (2010). Turbulent dispersed multiphase flow. *Annual Review of Fluid Mechanics*, 42, 111-133.

Boes, R.M. and Hager, W.H. (2003). Two-phase flow characteristics of stepped spillways. *Journal of Hydraulic Engineering*, 129(9), 661-670.

Bombardelli, F.A. (2012). Computational multi-phase fluid dynamics to address flows past hydraulic structures. In: *Proc. 4th IAHR Intl. Symp. Hydraulic structures*, APRH – Associação Portuguesa dos Recursos Hídricos [Portuguese water resources association], J. Matos, S. Pagliara, I. Meireles, eds., 9–11 February, Porto, Portugal, 2-19.

Bung, D.B. (2011). Developing flow in skimming flow regime on embankment stepped spillways. *Journal of Hydraulic Research*, 49(5), 639-648.

Bung, D.B. and Valero, D., 2016, July. Image processing techniques for velocity estimation in highly aerated flows: bubble image velocimetry vs. optical flow. In: *Proc. 4th IAHR Europe Congress*, Liège, Belgium, 151-157.

Bung, D.B. and Valero, D. (2017). FlowCV-An open-source toolbox for computer vision applications in turbulent flows. In: *Proc. 37th IAHR World Congress*, Kuala Lumpur, Malaysia.

Cameron, S.M., Nikora, V.I. and Stewart, M.T. (2017). Very-large-scale motions in rough-bed open-channel flow. *Journal of Fluid Mechanics*, 814, 416-429.

Castro, A.M., Li, J. and Carrica, P.M., 2016. A mechanistic model of bubble entrainment in turbulent free surface flows. *International Journal of Multiphase Flow*, 86, 35-55.

Castro-Orgaz, O. (2010). Velocity Profile and Flow Resistance Models for Developing Chute Flow. *Journal of Hydraulic Engineering*, 136(7), 447-452.

Chanson, H. (1994). Hydraulics of skimming flows over stepped channels and spillways. *Journal of Hydraulic Research*, 32(3), 445-460.

Chanson, H. (1996). *Air bubble entrainment in free-surface turbulent shear flows*. Elsevier.

Chanson, H., (2009). Turbulent air–water flows in hydraulic structures: dynamic similarity and scale effects. *Environmental Fluid Mechanics*, 9(2), 125-142.

Chanson, H. (2013). Hydraulics of Aerated Flows: Qui Pro Quo?. *Journal of Hydraulic Research*, Vision Paper, 51(3), 223-243.

Chanson, H. and Brattberg, T. (2000). Experimental study of the air–water shear flow in a hydraulic jump. *International Journal of Multiphase Flow*, 26(4), 583-607.

Chanson, H. and Toombes, L. (2002). Air–water flows down stepped chutes: turbulence and flow structure observations. *International Journal of Multiphase Flow*, 28(11), 1737-1761.

Deane, G. B. and Stokes, M.D. (2002). Scale dependence of bubble creation mechanisms in breaking waves. *Nature*, 418(6900), 839.

Felder, S. and Chanson, H. (2016). Air–water flow characteristics in high-velocity free-surface flows with 50% void fraction. *International Journal of Multiphase Flow*, 85, 186-195.

Felder, S. and Chanson, H. (2017). Scale effects in microscopic air-water flow properties in high-velocity free-surface flows. *Experimental Thermal and Fluid Science*, 83, 19-36.

Johnson, E.D. and Cowen, E.A., 2016. Remote monitoring of volumetric discharge employing bathymetry determined from surface turbulence metrics. *Water Resources Research*, 52(3), 2178-2193.

Kramer, M. and Chanson, H. (2018). Transition flow regime on stepped spillways: air–water flow characteristics and step-cavity fluctuations. *Environmental Fluid Mechanics*, 1-19.

Kramer, M., Chanson, H. and Felder, S. (2019a). Can we improve the non-intrusive characterization of high-velocity air–water flows? Application of LIDAR technology to stepped spillways. *Journal of Hydraulic Research*, 1-13.

Kramer, M., Valero, D., Chanson, H. and Bung, D.B. (2019b). Towards reliable turbulence estimations with phase-detection probes: an adaptive window cross-correlation technique. *Experiments in Fluids*, 60(1), 2.

Kolmogorov, A.N. (1941). The Local Structure of Turbulence in Incompressible Viscous Fluid for Very Large Reynolds Numbers. *Dokl. Akad. Nauk SSSR*, 30, 299-303. (In Russian)

Langevin, P. (1908). Sur la théorie du movement Brownien. *Comptes Rendus Acad. Sci*., 146, 530-533.

Murzyn, F., Mouaze, D. and Chaplin, J.R. (2005). Optical fibre probe measurements of bubbly flow in hydraulic jumps. *International Journal of Multiphase Flow*, 31(1), 141-154.

Nezu, I. (1977). *Turbulent Structure in Open-Channel Flows*. PhD thesis, Kyoto University.

Nezu, I. and Rodi, W. (1986). Open-channel flow measurements with a laser Doppler anemometer. *Journal of Hydraulic Engineering*, 112(5), 335-355.

Pope, S.B. (2000). *Turbulent Flows*. Cambridge University Press.

Straub, L.G. and Anderson, A. G. (1958). Experiments on self-aerated flow in open channels. *Journal of the Hydraulics Division*, 84(7), 1-35.

Tennekes, H. and Lumley, J.L. (1972). *A first course in turbulence*. MIT Press.

Valero, D. (2018). *On the Fluid Mechanics of Self-Aeration in Open Channel Flows*. PhD thesis, Université de Liège.

Valero, D. and Bung, D.B. (2015). Hybrid investigations of air transport processes in moderately sloped stepped spillway flows. In: Proc. *36th IAHR World Congress*, The Hague, Netherlands.

Valero, D. and Bung, D.B. (2016). Development of the interfacial air layer in the non-aerated region of high-velocity spillway flows. Instabilities growth, entrapped air and influence on the self-aeration onset. *International Journal of Multiphase Flow*, 84, 66-74.

Valero, D. and Bung, D. B. (2018). Reformulating self-aeration in hydraulic structures: Turbulent growth of free surface perturbations leading to air entrainment. *International Journal of Multiphase Flow*, 100, 127-142.

Valero, D. and García-Bartual, R. (2016). Calibration of an air entrainment model for CFD spillway applications. In *Advances in hydroinformatics*, 571-582. Springer, Singapore.

Wang, H., Murzyn, F. and Chanson, H. (2015). Interaction between free-surface, two-phase flow and total pressure in hydraulic jump. *Experimental Thermal and Fluid Science*, 64, 30-41.

Wei, W., Deng, J. and Zhang, F. (2016). Development of self-aeration process for supercritical chute flows. *International Journal of Multiphase Flow*, 79, 172-180.

Wood, I.R. (1984). Air Entrainment in High Speed Flows. In: *Symposium on Scale Effects in Modelling Hydraulic Structures*, (Ed.: H. Kobus) Esslingen am Neckar, Germany.

Zhang, G. and Chanson, H. (2018). Application of local optical flow methods to high-velocity free-surface flows: Validation and application to stepped chutes. *Experimental Thermal and Fluid Science*, 90, 186-199.